Cancer Cell
Article

Modeling of C/EBPα Mutant Acute Myeloid Leukemia Reveals a Common Expression Signature of Committed Myeloid Leukemia-Initiating Cells

Peggy Kirstetter,[1,8] Mikkel B. Schuster,[1,2,8] Oksana Bereshchenko,[1] Susan Moore,[1] Heidi Dvinge,[3] Elke Kurz,[1] Kim Theilgaard-Mönch,[2] Robert Månsson,[4] Thomas Å. Pedersen,[1] Thomas Pabst,[5] Evelin Schrock,[6] Bo T. Porse,[2] Sten Eirik W. Jacobsen,[4] Paul Bertone,[3] Daniel G. Tenen,[7] and Claus Nerlov[1,*]

[1]European Molecular Biology Laboratory, Mouse Biology Unit, Monterotondo 00016, Italy
[2]Laboratory for Gene Therapy Research, Copenhagen University Hospital, 2100 Copenhagen, Denmark
[3]European Bioinformatics Institute, Wellcome Trust Genome Campus, Cambridge CB10 1SD, UK
[4]Hematopoietic Stem Cell Laboratory, Lund Strategic Center for Stem Cell Biology and Cell Therapy, University of Lund, 22184 Lund, Sweden
[5]Institute of Medical Oncology, University Hospital, Bern 3010, Switzerland
[6]Institute for Clinical Genetics, Dresden University of Technology, 01307 Dresden, Germany
[7]Harvard Institutes of Medicine, Boston, MA 02115, USA
[8]These authors contributed equally to this work.
*Correspondence: nerlov@embl.it
DOI 10.1016/j.ccr.2008.02.008

SUMMARY

Mutations in the *CEBPA* gene are present in 7%–10% of human patients with acute myeloid leukemia (AML). However, no genetic models exist that demonstrate their etiological relevance. To mimic the most common mutations affecting *CEBPA*—that is, those leading to loss of the 42 kDa C/EBPα isoform (p42) while retaining the 30kDa isoform (p30)—we modified the mouse *Cebpa* locus to express only p30. p30 supported the formation of granulocyte-macrophage progenitors. However, p42 was required for control of myeloid progenitor proliferation, and p42-deficient mice developed AML with complete penetrance. p42-deficient leukemia could be transferred by a Mac1$^+$c-Kit$^+$ population that gave rise only to myeloid cells in recipient mice. Expression profiling of this population against normal Mac1$^+$c-Kit$^+$ progenitors revealed a signature shared with MLL-AF9-transformed AML.

INTRODUCTION

AML is a disease that has been found to reside in a self-renewing population of cancer stem cells—that is, leukemia-initiating cells (LICs). By transplantation of fractionated cells from patients with AML into SCID mouse recipients, a population of CD34$^+$CD38$^-$ LICs were identified in patients with diverse AML subtypes (Bonnet and Dick, 1997; Lapidot et al., 1994). These cells, which may comprise only a small fraction of the tumor cells, share surface markers with human repopulating hematopoietic stem cells, and were found to give rise to the bulk of non-LIC tumor cells through a differentiation hierarchy analogous to that of normal hematopoiesis. Recently, however, an alternative hypothesis to the hematopoietic stem cell (HSC)-like LIC has been developed. By transduction of mouse bone marrow (BM) cells with oncogenic fusion proteins (MLL-ENL and MOZ-TIF2), transformation of phenotypic HSCs, as well as committed myeloid progenitors (common myeloid progenitor [CMP] and granulocyte-macrophage progenitor [GMP]) has been achieved (Cozzio et al., 2003; Huntly et al., 2004; Somervaille and Cleary, 2006). The resulting LICs display characteristics of committed myeloid progenitors and give rise to nonleukemogenic progeny in

SIGNIFICANCE

These results demonstrate that, in a mouse model, patient-derived *CEBPA* mutations are AML-initiating mutations, providing direct genetic validation of their etiological importance. Furthermore, we show that at the cellular level such mutations uncouple myeloid lineage commitment from progenitor proliferation control, leading to the transformation of committed myeloid progenitor cells. Committed myeloid leukemia-initiating cells (LICs) have been derived in vitro through ectopic expression of translocation-derived oncogenic fusion proteins. We find that unbiased interrogation of the hematopoietic hierarchy by an endogenous leukemia-initiating mutation can transform a committed AML-LIC and can identify a gene expression profile shared between progenitors transformed by *Cebpa* mutation and MLL-AF9 overexpression, respectively, indicating a conserved molecular basis for committed LIC transformation.

a myeloid-restricted hierarchy. Interestingly, in the case of MLL-AF9-transformed GMP-like LICs, the upregulation of a gene subset normally restricted to HSCs was observed (Krivtsov et al., 2006), raising the possibility that reactivation of an HSC-associated self-renewal program is involved in the generation of ectopically self-renewing progenitors. However, because such myeloid-committed LICs have so far been generated only through retroviral transduction and the resulting oncoprotein overexpression, some key questions remain to be answered. First, will the hematopoietic hierarchy, when interrogated by an endogenous initiator mutation, generate such committed progenitors? Second, because elements of the MLL-AF9 HSC-like signature was present in human leukemias with *MLL* translocations, but not in non-*MLL* AML (Krivtsov et al., 2006), is reactivation of an HSC self-renewal program a general mechanism for progenitor transformation, or do other self-renewal programs exist that are able to maintain myeloid-committed LICs?

Mutations in the *CEBPA* gene, encoding the C/EBPα transcription factor, are observed in ~9% of de novo AML cases and typically involve mutation of both *CEBPA* alleles (Nerlov, 2004). There is evidence that *CEBPA* mutations are early events in the generation of leukemic clones, because, in the vast majority of cases, patients undergoing relapse of AML display the same mutations in both *CEBPA* alleles as they did before complete remission (Shih et al., 2006; Tiesmeier et al., 2003), indicating that these mutations are present already in early leukemic or preleukemic cell populations. In comparison, *FLT3* mutation status is different in ~30% of patients with AML at the time of relapse, and mutations may be present in only a subset of leukemic blasts, consistent with a role in disease progression (Kottaridis et al., 2002; Shih et al., 2002). C/EBPα is produced as two major polypeptides of 42 kDa (p42) and 30 kDa (p30), respectively, generated by alternative translation initiation (Lin et al., 1993). The most common *CEBPA* mutation found in patients with AML involves the selective loss of p42 expression due to frameshift mutations in the part of the coding sequence unique to this isoform (Leroy et al., 2005), a mutation also found in familial AML pedigrees (Sellick et al., 2005; Smith et al., 2004).

Studies of C/EBPα knockout mice have demonstrated defects in adipogenesis, granulopoiesis, and liver metabolism (Wang et al., 1995; Zhang et al., 1997), the last of which leads to perinatal lethality. More recently, a requirement for C/EBPα in the formation of early bipotent GMPs from the CMP was demonstrated (Heath et al., 2004; Zhang et al., 2004). These studies did not show development of AML in the absence of C/EBPα, most likely because of the early block in myeloid lineage commitment. However, because those experiments involve deletion of the entire C/EBPα coding sequence, they do not accurately model *CEBPA* alleles found in patients, where null mutations rarely, if ever, occur (Nerlov, 2004). To more accurately model human AML-derived *CEBPA* mutations and to determine the individual roles of p42 and p30 in GMP formation, proliferation control, and myeloid tumor suppression, we generated knockin mice in which p42 translation is specifically ablated. In the absence of p42, GMPs were still formed; however, the resulting myeloid progenitors had vastly increased self-renewal capacity, and mice uniformly progressed to AML and died with combined liver and bone marrow failure. The disease could be transplanted in the absence of detectable phenotypic HSCs but was efficiently transferred by $Mac1^+c\text{-}Kit^+$ committed myeloid cells. Gene profiling of p42-deficient LICs against normal $Mac1^+c\text{-}Kit^+$ cells identified a gene expression signature overlapping that reported for MLL-AF9-transformed GMPs but, to a lesser extent, containing the self-renewal signature shared by HSCs and MLL-AF9-transformed cells. These results show that (1) loss of p42 uncouples myeloid lineage commitment from progenitor proliferation control, leading to myeloid lineage transformation; (2) unbiased interrogation of the hematopoietic system by an endogenous leukemia-initiating mutation may lead to the generation of committed myeloid LICs; and (3) committed progenitors transformed by distinct initiating mutations may share a transformation-specific gene expression signature.

RESULTS

To disrupt translation of p42 from the mouse *Cebpa* gene, we placed a LoxP-flanked neomycin resistance cassette site in the *Cebpa* locus between the p42 and p30 initiation codons (Figure 1A, LNLp30 allele). Upon Cre-mediated deletion of the cassette, the remaining LoxP site introduced a nonsense codon into the p42-specific part of the C/EBPα encoding open reading frame (Lp30 allele), leading to termination of translation initiated at the p42 AUG, without interfering with translation initiated at the p30 AUG (Figure 1B). The LNLp30 allele was introduced into the mouse *Cebpa* locus by homologous recombination in E14.1 ES cells. Germline transmission was obtained from 2 independent ES cell clones. By crossing mice carrying the LNLp30 allele to the deleter-Cre line, mice heterozygous for the Lp30 allele were obtained. These $Cebpa^{Lp30/+}$ mice (henceforth "L/+ mice") displayed no obvious phenotype in hepatic, hematopoietic, or adipose tissues, and both sexes were fertile. Intercrosses between L/+ mice gave rise to homozygous L/L mice. However, analysis of 17 litters showed that although +/+ (28/89) and L/+ mice (57/89) were observed at weaning at the expected Mendelian ratio of 1:2, only 4/89 mice with a L/L genotype were retrieved, about 14% of the expected number. Immediately after birth, the L/L genotype was observed at the Mendelian ratio (Figure 1C), indicating significant perinatal lethality in the complete absence of C/EBPα p42, but less severe than that resulting from a *Cebpa* null mutation (Wang et al., 1995). The phenotype of newborn L/L mice was consistent with hypoglycemia being the cause of perinatal death; however, the detailed metabolic phenotype observed in the absence of p42 will be described elsewhere (authors' unpublished data). Specific loss of C/EBPα p42 in L/L mice was confirmed by western blot analysis of liver nuclear lysates (Figure 1D); this analysis also showed that in L/+ mice the p42/p30 ratio in the liver was decreased by 2.5 fold in L/+ mice, relative to +/+ controls (Figure 1E). It is interesting to note that disruption of p42 translation leads to an increase in the level of p30; this is similar to what is observed in samples from human patients with AML (Pabst et al., 2001). Surviving L/L mice were observed to live for up to a year, and both sexes were fertile. Thus, although C/EBPα p42 was required for efficient perinatal survival, C/EBPα p30 is sufficient for sustaining fertile life after the perinatal period.

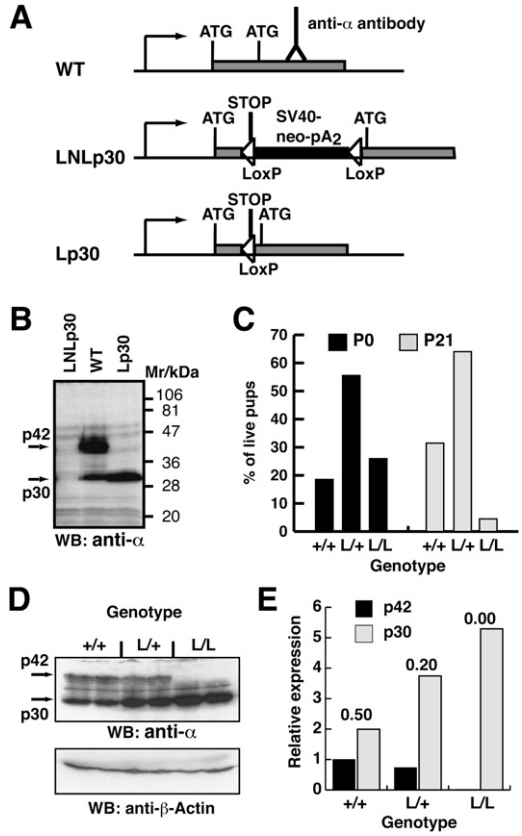

Figure 1. Generation of p42 Knockout Mice

(A) Schematic representation of the targeting strategy used to generate the Lp30 allele. The location of the ATG codons initiating p42 and p30, and the epitope recognized by the anti-C/EBPα antibody, are shown.

(B) Western blot analysis of C/EBPα levels in total lysates of Q2bn cells transiently transfected with pCMV-αLNLp30 (lane 1), pCMV-αWT (lane 2), and pCMV-αLp30 (lane 3), respectively. The positions of the p42 and p30 are indicated.

(C) The percentage of pups retrieved from L/+ intercrosses with +/+, L/+, and L/L genotypes at birth (P0; n = 28) and at weaning (P21; n = 89).

(D) Western blot analysis of C/EBPα-actin and β-actin levels in nuclear lysates from livers of WT (lanes 1–2), L/+ (lanes 3–4), or L/L mice (lanes 5–6).

(E) Bar graph showing the levels of p42 (black bars) and p30 (gray bars), respectively, normalized to β-actin levels. The levels were determined by densitometric analysis of the western blots shown in (D). Numbers above the bars show the p42/p30 ratio for the different genotypes.

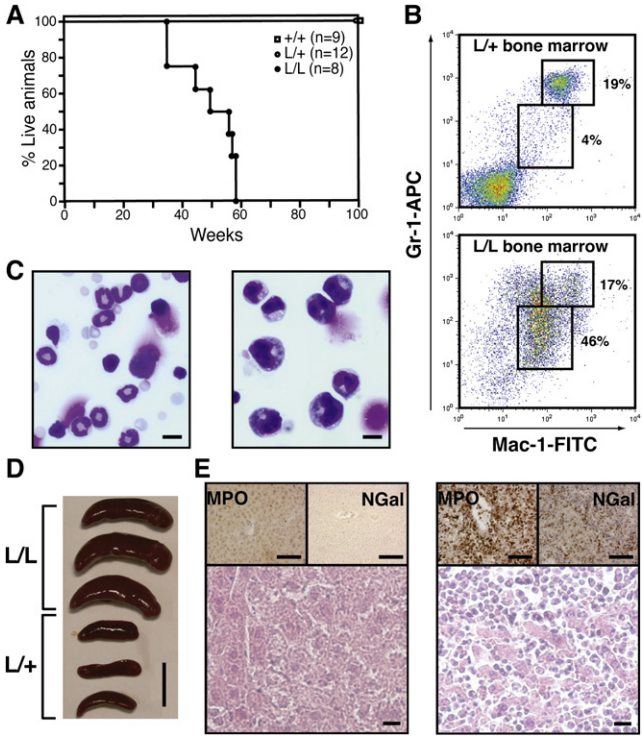

Figure 2. AML in the Absence of p42

(A) Kaplan-Meier plot showing latency to death or moribund state for the +/+, L/+, and L/L genotypes. Significance of decreased survival of L/L mice versus that of L/+ or +/+ mice is indicated.

(B) Staining of littermate control BM (L/+; upper panel) and BM from moribund L/L mice (lower panel) using anti-Mac-1-FITC and anti-Gr-1-APC. Note the accumulation of Mac-1^{+},Gr-1^{lo} immature granulocytic cells in the L/L BM (lower gate), whereas the normal granulocytes are Mac-1^{+},Gr-1^{hi} (upper gate).

(C) Cytospin of BM from L/+ (left panel) and leukemic L/L (right panel) mice, stained with May-Grünwald-Giemsa. Scale bar, 10 μm.

(D) Spleens of L/L (top) and L/+ (bottom) mice at 30 weeks of age. Scale bar, 1 cm.

(E) Large frame: liver section of L/+ (left panels) and moribund L/L (right panels) mice stained with hematoxylin-eosin. Insets: sections of the same liver stained for MPO and NGal, respectively. Scale bars: main figure, 10 μm; left insets, 100 μm; and right insets, 200 μm.

Aberrant Granulopoiesis and Progression to AML in Mice Lacking p42

AML mutations preventing p42 translation have been reported in both the presence and absence of mutation of the second *CEBPA* allele (Leroy et al., 2005; Nerlov, 2004). To determine whether *Cebpa* alleles that are unable to translate p42 affect myeloid differentiation in the monoallelic state, we analyzed +/+ and L/+ mice at various ages for symptoms of hematological malignancy. L/+ mice were maintained for 18 months without mortality or alterations in hematopoietic tissues or granulocyte differentiation profile, compared with +/+ controls (see Figure S1 available online). In contrast, L/L mice became anemic and moribund or died after 9–14 months (Figure 2A). Necropsy revealed BM failure, where normal hematopoietic cells were replaced by Mac-1^{+}Gr-1^{lo} cells with high myeloid blast count (>30%; Figures 2B and 2C). Spleens were highly enlarged (Figure 2D), and livers contained massive hematopoietic infiltrates; the remaining hepatocytes were few and scattered (Figure 2E). Immunohistochemistry revealed myeloperoxidase (MPO) and NGal-positive granulocytic cells infiltrating the tissue (Figure 2E, insets). This analysis indicated that L/L mice uniformly developed AML, with combined liver and BM failure as the likely cause of death.

Analysis of L/L mice before hematological collapse (<8 months) showed the presence of several age-dependent phenotypes: in young mice (<2 months), a neutropenic BM (i.e., L/L-1 phenotype, low number of Mac1^{+}Gr1^{+} cells [Figures 3A and 3D], normal level of c-Kit^{+} cells [Figure 3B], and few granulocytic cells by morphology [Figure 3C]) was the most common observation. The peripheral blood also contained lower numbers of myeloid cells Figure S4A). This phenotype uniformly progressed to granulocyte lineage transformation by 6 months (L/L-3 phenotype; increase of c-Kit^{+} cells [Figures 3B and 3D] and

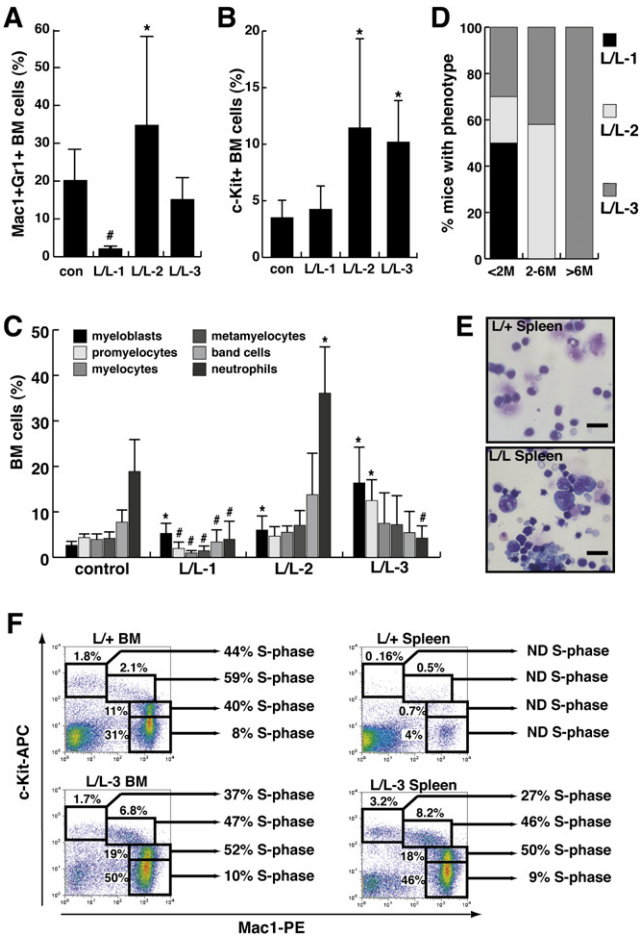

Figure 3. Disease Progression of L/L Mice

(A) Number of Mac-1$^+$Gr-1$^+$ cells determined by flow cytometry performed on bone marrow cells from control (L/+) mice and L/L mice characterized by neutropenia (L/L-1 phenotype; n = 5), granulocyte hyperproliferation (L/L-2 phenotype; n = 4), and transformation (L/L-3 phenotype, n = 5), respectively. Values significantly higher (*) and lower (#) than control values are indicated ($p < 0.05$). Error bars = standard deviation (SD).

(B) Representation of c-Kit positive cells determined by flow cytometry performed on the same bone marrow cells as in (A). Error bars = SD.

(C) Representation of different maturation stages of myeloid cells in bone marrow from control (+/+, L/+; n = 6), L/L-1 (n = 5), L/L-2 (n = 4), and L/L-3 mice (n = 5), determined by differential counts performed on May-Grünwald Giemsa-stained cytospins. Values significantly higher (*) and lower (#) than control values are indicated ($p < 0.05$). Error bars = SD.

(D) Distribution of the 3 L/L phenotypes in mice <2 months (n = 10), 2–6 months (n = 7), and >6 months old (n = 12), respectively.

(E) Cytospin of splenocytes from L/+ and L/L-3 mice stained with May-Grünwald -Giemsa. Scale bar, 20 μm.

(F) Analysis of myeloid cell proliferation in BM and spleen of L/+ and L/L-3 mice. Mice were injected intraperitoneally with BrdU 2 hr before death. Cells were stained for expression of c-Kit and Mac-1, as well as for BrdU incorporation. The amount of BrdU-positive S-phase cells in the Mac-1$^-$c-Kit^{hi}, Mac-1$^+$c-Kit^{hi}, Mac-1^{hi}c-Kit$^+$ and Mac-1^{hi}c-Kit$^-$ fractions (top left to bottom right) are indicated. ND: no BrdU staining detectable above the negative control staining.

accumulation of myeloblasts/promyelocytes and block in granulocyte differentiation [Figure 3C]), with granulocyte hyperproliferation (L/L-2 phenotype; high levels of Mac1$^+$Gr1$^+$ mature granulocytes) as a possible intermediate stage (Figures 3C and 3D). Parallel changes in granulocyte numbers were observed in the spleen (Figure S2). The differentiation profile of the erythroid lineage was not altered (Figure S3); however, at late stages of disease, normal hematopoiesis was displaced by malignant myeloid cells, leading to decreased hematocrit and leukocyte count (Figures S4E–S4H). These results showed that loss of p42 leads to myeloid lineage transformation. This phenotypic progression is similar to that observed in mice containing a point mutation in the C/EBPα basic region that disables C/EBPα-mediated E2F repression and cell cycle control (BRM2 mice) (Porse et al., 2005), with the important difference that L/L mice develop malignant disease, whereas BRM2 mice do not. We therefore focused on the malignant L/L-3 phenotype. In L/L-3 mice, the spleen also contained high levels of myeloid blasts (Figure 2E), indicative of ectopic myelopoiesis. We therefore analyzed the presence of proliferating myeloid cells in BM and spleen of L/L-3 and control L/+ mice by in vivo BrdU pulse-labeling. This analysis showed that both L/L-3 BM and spleen contained increased numbers of proliferating Mac-1$^+$c-Kit$^+$ cells, compared with L/+ controls (Figure 3F). This was particularly significant in the case of the spleen, because it normally contains differentiated neutrophils and macrophages and few progenitors. We did not observe any karyotypic abnormalities in tumor cells from three leukemic mice, by use of spectral karyotyping (SKY), with the exception of one case of loss of the Y chromosome (Figure S5). Loss of the Y chromosome is common in human AML and does not have any detectable effect on prognosis (Wiktor et al., 2000). These results are consistent with the observation that *CEBPA* mutant AML is most commonly karyotypically normal (Frohling et al., 2004).

Ectopic Proliferation and Increased Self-Renewal of Myeloid Progenitors in the Absence of C/EBPα p42

It has previously been observed that deletion of the C/EBPα gene leads to an increase in the proliferative capacity of progenitors but that this increase does not lead to AML, most likely because of the requirement for C/EBPα in myeloid lineage commitment at the CMP-GMP transition (Heath et al., 2004; Zhang et al., 2004). We therefore analyzed the presence of GMPs and the self-renewal capacity of progenitors in mice lacking p42 before BM transformation. GMPs were still formed in L/L-1 mice (Figure 4A), showing that p30 is sufficient to mediate the CMP-GMP commitment step. However, L/+ BM myeloid progenitors showed mildly increased proliferative capacity, compared with +/+ progenitors, and L/L-1 progenitors were highly proliferative with frequent spontaneous immortalization (Figure 4B and data not shown). The long-term myeloid cultures derived from L/L-1 mice contained mainly Mac-1$^+$c-Kit$^+$ cells (Figure 4C), which were dependent on stem cell factor (SCF) and interleukin (IL)-3 for survival (Figure 4D). To determine whether the increased self-renewal capacity was specifically present in committed myeloid cells, we sorted Lin$^-$Sca-1$^+$c-Kit$^+$ (LSK) stem−/pluripotent cells, GMPs, and megakaryocyte-erythoid progenitor (MEP) populations from L/L-1, L/+, and +/+ mice. MEPs generated only primary colonies in all genotypes (Figure 4E), whereas L/L GMPs replated over >5 passages, consistent with the data obtained with total BM (Figure 4F). When LSK cells were replated, initial replating efficiencies were similar in all genotypes. However, at the fourth

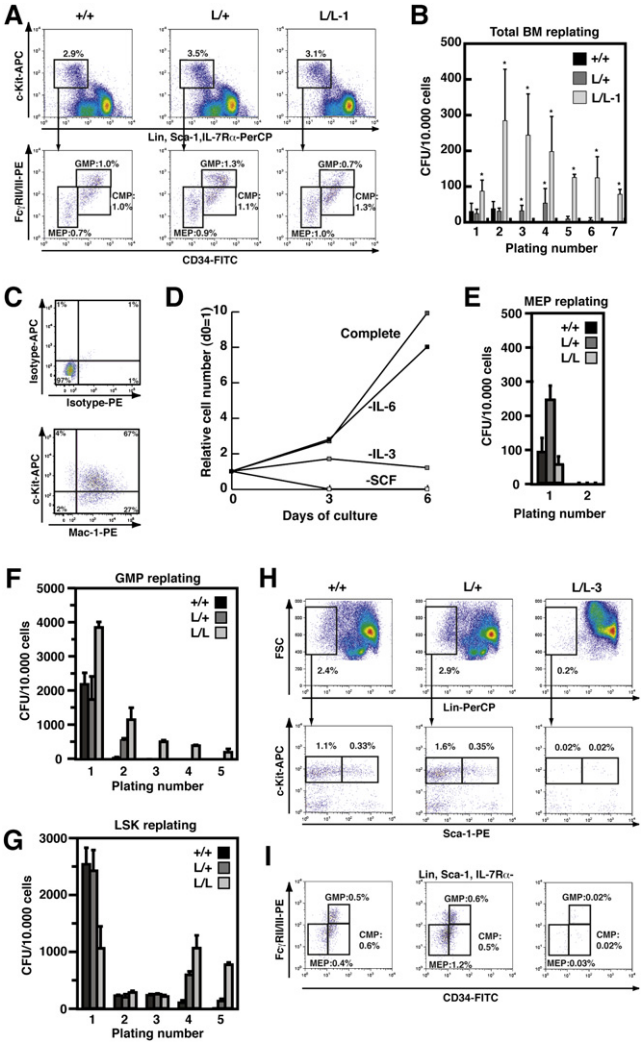

Figure 4. Progenitor Phenotype of L/L Mice

(A) Analysis of myeloid progenitor populations in young (7 weeks) +/+, L/+, and L/L-1 mice. The CMP, GMP, and MEP populations in BM were determined by flow cytometry. The size of the CMP, GMP, and MEP populations is shown as the percentage of total BM cells. These results are representative of three determinations.

(B) Replating efficiency of myeloid progenitors from +/+ (n = 4), L/+ (n = 6), and L/L-1 (n = 7) mice. Ten thousand BM cells were plated in M3434 medium, and colonies counted after 1 week. The same number of cells was replated in M3434 medium. This procedure was repeated six times. The average number of colonies from triplicate cultures for each mouse is shown. An asterisk (*) indicates a value significantly higher than the +/+ value ($p < 0.05$). Error bars = SD.

(C) Immortalized L/L BM cells were stained with anti-c-Kit-APC and anti-Mac-1-PE (lower panel) or corresponding isotype control antibodies (upper panel) and were analyzed by flow cytometry. The percentage of cells in the four quadrants is indicated.

(D) Immortalized L/L BM cells were cultured in the presence of SCF, IL-3, and IL-6 (complete medium), or in the absence of one of these factors, as indicated. The number of live cells was counted at 3 day intervals, and the average of three determinations is shown, normalized to the initial cell number (= 1).

(E) MEPs sorted from +/+, L/+, and L/L-1 mice (initial plating, 900 cells/dish) were replated in M3434 medium as in (B). Error bars = SD.

(F) GMPs sorted from +/+, L/+, and L/L-1 mice (initial plating, 250 cells/dish) were replated in M3434 medium as in (B). Error bars = SD.

plating, the pattern from the GMP replating reemerged (L/+ mildly and L/L-1 strongly increased over +/+), indicating that increased replating/self-renewal occurring once the pluripotent/stem cells reach the committed myeloid progenitor stage (Figure 4G). Indeed, cultures at this stage contained only Mac1$^+$ cells (data not shown). Before transformation, no change in levels of LSK stem$^-$/pluripotent cells (Figure S6) or BM myeloid progenitors (Figure 4A) was observed in L/L-1 BM, compared with controls. However, after transformation (L/L-3 mice), the BM LSK compartment (Figure 4H) as well as the committed myeloid CMP, GMP, and MEP populations (Figure 4I) were virtually absent. C/EBPα p30 is therefore sufficient for commitment of CMPs to a myeloid fate, whereas p42 is required to control the proliferation of myeloid progenitors. In its absence, the myeloid lineage transforms and eventually expands, leading to displacement of the normal stem cell/progenitor compartment.

p42-Deficient AML Is Transplantable in the Absence of Phenotypic HSCs

The vastly increased ability of p42-deficient myeloid progenitors to proliferate, combined with the decrease in LSK, CMP, and GMP populations, indicated a committed myeloid progenitor as a likely target of transformation. To determine whether the resulting tumors indeed contained myeloid cells capable of initiating leukemia, L/L-3 BM cells (CD45.2 allotype) containing very low levels of LSK cells (Figure 5A) were enriched for Mac-1$^+$ cells by immunomagnetic separation. At this point, LSK cells were undetectable (data not shown). One hundred thousand such cells were competitively transplanted into lethally irradiated CD45.1 recipients, along with 400,000 CD45.1/2 wild-type (WT) BM cells to provide radioprotection and competition. Control mice received 100,000 cells from L/+ BM and 400,000 CD45.1/2 competitor BM cells. L/L-transplanted mice developed leukopenia and anemia (Figure 5B) and became moribund or died within 9–18 weeks (Figure 5C), whereas no leukemia or lethality was observed in L/+ transplanted mice. Analysis of BM and spleen from moribund mice showed that normal hematopoiesis was largely displaced by CD45.2 cells that expressed Mac-1 or c-Kit (Figure 5D) and were devoid of LSK cells (Figure 5E).

This result was consistent with a non-HSC phenotype of the LIC. To further address this possibility, we sorted leukemic L/L-3 and normal L/+ BM cells into four fractions, using a lineage cocktail without anti-Mac-1 and anti-Gr-1 (Lin*): Lin*$^-$Sca-1$^+$ cells (fraction A, containing the HSC compartment), Lin*$^-$Mac-1$^-$Sca-1$^-$c-Kit$^+$ (fraction B: containing the CMP/GMP/MEP compartment), Lin*$^-$Mac-1$^+$c-Kit$^+$ (fraction C: containing committed myeloid progenitors), and Lin*$^-$Mac-1$^+$c-Kit$^{lo/-}$ (fraction D,

(G) LSK cells sorted from +/+, L/+, and L/L-1 mice (initial plating, 120 cells/dish) were replated in M3434 medium as in (B). Error bars = SD.

(H) Analysis of the LSK compartment in transformed (L/L-3) mice and +/+ and L/+ controls. The size of the LSK (right) and Lin-Sca-1-c-Kit+ (left) populations is shown as a percentage of total BM cells. Results are representative of four determinations.

(I) Analysis of the myeloid progenitor compartments in transformed (L/L-3) mice and +/+ and L/+ controls. The size of the CMP, GMP, and MEP populations is shown as a percentage of total BM cells. Results are representative of four determinations.

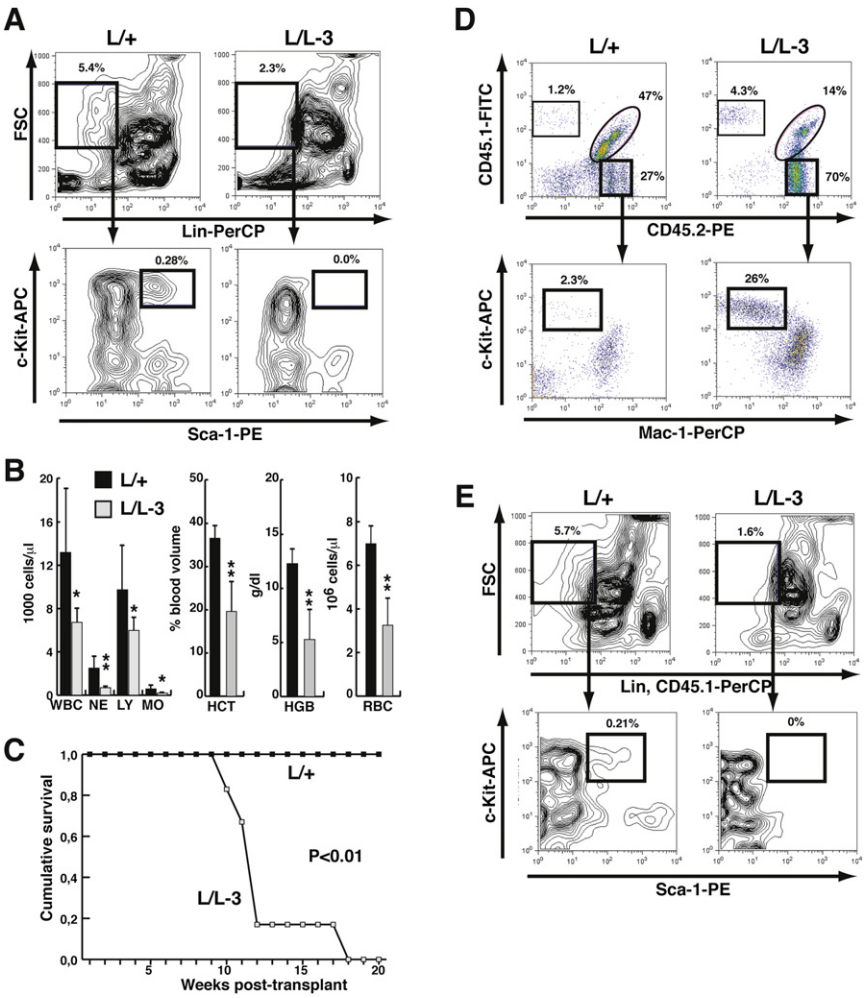

Figure 5. p42 Knockout Leukemia Is Transplantable

(A) Immunophenotype of L/+ and L/L-3 BM used for transplantation. The percentages of $Lin^{-/lo}$ and LSK cells of total BM cells are indicated.

(B) Analysis of peripheral blood of transplanted mice 9 weeks after transplantation (L/+ [n = 6], black bars; L/L-3 [n = 6], gray bars). The numbers of leukocytes (WBC: total leukocytes; NE: neutrophils; LY: lymphocytes; MO: monocytes), red blood cells (RBC), hematocrit (HCT), and hemoglobin (HGB) values are shown. Asterisks indicate significant difference from L/+ controls (*$p < 0.05$; **$p < 0.001$). Error bars = SD.

(C) Kaplan-Meier plot of mice transplanted with Mac-1-enriched leukemic L/L-3 BM or control L/+ BM cells (n = 6 for both groups). Significance of decreased survival of L/L-3 versus L/+ transplanted mice is indicated.

(D) BM from L/+ and L/L-3 transplanted mice was stained with CD45.1-FITC and CD45.2-PE, to identify donor CD45.2 cells, and with Mac-1-PerCP and c-Kit-APC, to determine the number of myeloid cells and c-Kit+ progenitors. Percentages indicate the proportion of gated populations.

(E) Immunophenotype of BM cells of mice transplanted with L/+ and L/L BM cells. Cells were stained with biotinylated lineage cocktail in which anti-CD45.1-bio was included to eliminate CD45.1 host and CD45.1/2 competitor cells from the $Lin^{-/lo}$ compartment, followed by Sav-PerCP, anti-Sca-1-PE, and anti-c-Kit-APC. The proportion of $Lin,CD45.1^{-/lo}$ and LSK cells are indicated as percentage of the total cell population.

containing differentiated myeloid cells) (Figure 6A). Two thousand cells of each fraction (CD45.2 allotype) were transplanted into lethally irradiated CD45.1 recipients, along with 250,000 WT CD45.1/2 competitor cells. Monitoring of peripheral blood chimerism showed, as expected, only the HSCs containing fraction A from L/+ BM engrafted mice (6/6 recipients). In contrast, the leukemic BM engraftment was observed only in mice transplanted with fraction C containing the committed myeloid cells (Figure 6B). Analysis of CD45.2 PB cells showed multilineage engraftment in L/+ mice, whereas in L/L-3 transplanted mice, engraftment was restricted to the myeloid lineage (Figure 6C; 6/6 recipients), consistent with the leukemia-initiating population being myeloid committed. Analysis of BM from transplanted mice confirmed that repopulation was restricted to fraction A for L/+ donors and to fraction C for L/L-3 donors, whereas engraftment of the CD45.1/2 competitor cells was seen in all recipients (Figure 6D). Also in BM, the L/L-3 fraction C engraftment was myeloid restricted (Figure 6E), and HSC engraftment (measured as $CD45.2^{+}CD45.1^{-}$ donor LSK cells) was seen only in the L/+ fraction A-transplanted mice (Figure 6F). Finally, high levels of $Mac\text{-}1^{+}c\text{-}Kit^{+}$ cells (fraction C phenotype) could be retrieved from L/L-3 fraction C recipients (Figure 6G). These cells gave rise to malignant disease upon retransplantation (data not shown).

Gene Expression Signature of p42-Deficient LIC

The fraction C containing the LIC population was isolated from three independently transplanted L/L-3 recipients and was compared by gene profiling to normal $Mac\text{-}1^{+}c\text{-}Kit^{+}$ progenitors from L/+ control mice. This provided an expression signature for the LL-LIC, consisting of both upregulated (388 probe sets) and downregulated genes (444 probe sets; false discovery rate [FDR] = 0.01; Table S1). Among these we confirmed upregulation of the surface antigen CD34 and downregulation of CD24 by flow cytometric analysis (Figure 7A). Also, the regulation of a number of potentially relevant genes was confirmed by Q-PCR: *Mef2C*, *Klf4*, *Ccnd2* were downregulated in LL-LICs, compared with normal progenitors, with a similar trend for *Ccnd1*, whereas *Ddit3* (encoding CHOP, a negative regulator of canonical C/EBPs) and the antiapoptotic gene *Bcl2a1a* were upregulated (Figure 7B). In addition to upregulation of *Ddit3*, downregulation of *Cebpb* was observed, indicating additional dysregulation of the C/EBP complex.

Of particular interest was the downregulation of *Mef2c*, *HoxA9*, and *Meis1* in LL-LIC: these genes are part of the L-GMP HSC-like signature. *Mef2C* was demonstrated to be functionally important for L-GMPs through RNAi knockdown (Krivtsov et al., 2006), and *Hoxa9* and *Meis1* are essential for

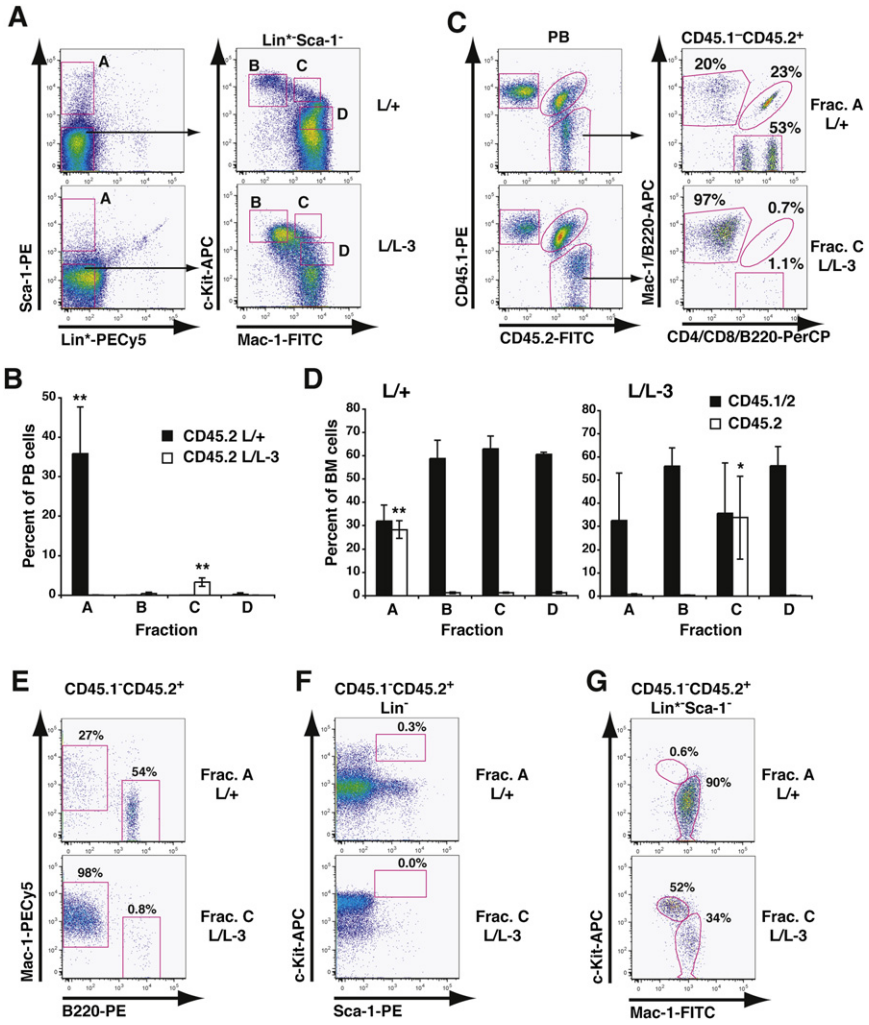

Figure 6. Mac1$^+$c-Kit$^+$ Committed Myeloid Progenitors Initiate p42 Knockout Leukemia

(A) Cell sorting strategy used to isolate fractions A (Lin^{*-}Sca-1$^+$), B (Lin^{*-}Sca-1$^-$c-Kit^{hi}Mac-1$^-$), C (Lin^{*-}Sca-1$^-$Mac1$^+$c-Kit$^+$), and D (Lin^{*-}Sca-1$^-$Mac1$^+$c-Kit$^-$) from L/+ (upper panels) and L/L-3 mice (lower panels).

(B) PB engraftment of donor-derived cells (CD45.2) 12 weeks after competitive transplantation of 2 × 10^3 bone marrow cells (CD45.2) from fractions A, B, C, and D of L/+ or L/L-3 mice with 2.5 × 10^5 competitor cells (CD45.1/2). Allotypes were determined by flow cytometry on PB mononuclear cells using anti-CD45.1-PE and anti-CD45.1-FITC antibodies (n = 5 mice/fraction). **p < 0.001, versus all other fractions. Error bars = SD.

(C) Representative dot plots of PB from L/+ fraction A (upper panel) and L/L-3 fraction C (lower panel) transplanted mice. Contribution of donor-derived cells (CD45.2) for myeloid cells (Mac-1$^+$), B cells (B220$^+$), and T cells (CD4/CD8$^+$). Percentages indicate the proportion of gated populations.

(D) BM engraftment of donor-derived cells (CD45.2) and competitor cells (CD45.1/2) 14 weeks after competitive transplantation of 2 × 10^3 bone marrow cells (CD45.2) fractions A, B, C, and D from L/+ or L/L-3 mice with 2.5 × 10^5 competitor cells (CD45.1/2). Allotypes were determined by flow cytometry on BM cells using anti-CD45.1-PE and anti-CD45.2-APC-Cy7 antibodies (n = 5 mice/fraction). **p < 0.001 and *p < 0.01, versus all other fractions. Error bars = SD.

(E) Immunophenotype CD45.1$^-$CD45.2$^+$ donor cells L/+ fraction A (upper panel) and L/L-3 fraction C (lower panel) was determined by staining with anti-Mac-1-PE-Cy5 and anti-B220-PE to identify myeloid and B-lineage cells. Percentages indicate the proportion of gated populations.

(F) The contribution of L/+ fraction A (upper panel) and L/L fraction C (lower panel) donor cells to the BM LSK compartment was analyzed. BM cells were stained with purified lineage cocktail (revealed with CyChrome-conjugated goat anti-rat antibody), Sca-1-PE, and c-kit-APC to determine LSK cells, and anti-CD45.1-PE-Cy5 and anti-CD45.2-FITC to identify CD45.1$^-$CD45.2$^+$ donor cells. Percentages indicate the proportion of total BM cells.

(G) Immunophenotype of BM from L/+ fraction A (upper panel) and L/L-3 fraction C (lower panel) transplanted mice stained with CD45.1-PE and CD45.2-APC-Cy7 to identified donor CD45.2$^+$ cells; BM cells were stained with biotinylated lineage cocktail (without anti-Mac1 and anti-Gr1) in which biotinylated anti-CD45.1 was included to eliminate CD45.1 host and CD45.1/2 competitor cells from the Lin$^{-/lo}$ compartment followed by Sav-PE-Cy5, Sca-1-PE-Cy7, and c-Kit-APC and Mac-1-FITC to determine myeloid progenitors. Percentages indicate the proportion of gated populations.

transformation by MLL fusion proteins (Ayton and Cleary, 2003; Wong et al., 2007). Their downregulation suggested that the molecular reprogramming of myeloid progenitors underlying LL-LIC transformation was distinct from that of the L-GMP. Indeed, of the 420 probe sets present in the L-GMP/HSC self-renewal signature, only 25 were present in the LL-LIC upregulated probe sets, versus 16 in the downregulated probe sets (Table S2), suggesting a limited overlap with the LL-LIC signature. We therefore proceeded to use the LL-LIC signatures to perform unsupervised hierarchical clustering of LL-LIC, L-GMP, and normal hematopoietic progenitors using our own as well as published gene expression profiles (Krivtsov et al., 2006). Using the combined signatures of both up- and downregulated genes from the LL-LIC profiling, the L-GMP and LL-LIC were found to cocluster (Figure S7), indicating that the L-GMP gene expression signature was related to the LL-LIC signature and suggesting the existence of a common progenitor transformation signature that is not dependent on the underlying initiating mutation. To confirm this and to identify this putative common signature, we next performed Gene Set Enrichment Analysis (GSEA). This algorithm may be used in a comparison between two sets of expression profiles to determine whether a particular expression signature is enriched or depleted (Subramanian et al., 2005). We used GSEA to determine whether the L-GMP expression profile was enriched in genes upregulated in LL-LICs or depleted of genes downregulated in this population, compared with normal GMPs. Both were found to be the case (Figure S8). There were 113 LL-LIC upregulated probe sets in enrichment core for L-GMPs, versus GMP ($p < 0.01$), and 159 downregulated probe in depletion core for L-GMPs, versus GMP ($p < 0.01$). A similar result was obtained in comparisons with the combined LSK, CMP, GMP, and MEP expression profiles (data not shown). Of the 113 probe sets accounting for the core enrichment of LL-LIC upregulated genes in L-GMP, 23 were shared with the

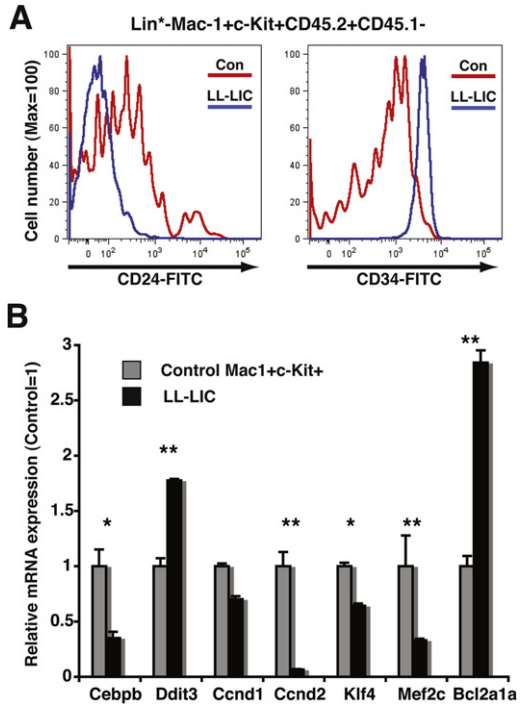

Figure 7. Profiling of LL-LIC

(A) Surface expression of CD24 and CD34 on Mac1$^+$c-Kit$^+$ progenitors was measured by flow cytometry on BM from CD45.1/2 recipients transplanted with L/L-3 fraction C (L/L-LIC) and L/+ fraction A cells (L/+ control) (CD45.2 allotype). The gated population was Lin*-c-Kit$^+$Mac-1$^+$CD45.1$^-$CD45.2$^+$.

(B) Quantitative real-time PCR analysis of gene expression in LL-LIC and L/+ fraction C cells. Cells were isolated from mice transplanted as in (A). Measurements are from three individually transplanted recipients, each performed in triplicate. Error bars indicate SD. *$p < 0.05$; **$p < 0.01$. Error bars = SD.

HSC-associated self-renewal signature, suggesting a significant, but limited, overlap between the two. The top 50 probe sets coenriched in L-GMP and LL-LIC are shown in Table 1.

DISCUSSION

The results presented here support several conclusions. First, our results genetically validate AML-associated *CEBPA* mutations as causative of AML and identify the separation of myeloid lineage commitment from progenitor proliferation control as a cellular mechanism underlying the oncogenic potential of mutations affecting C/EBPα. Second, we show that an endogenous leukemia-initiating mutation present throughout the hematopoietic hierarchy induces the generation of committed myeloid LICs. Third, we find that such transformation may occur with activation of a gene-expression program overlapping that induced by MLL-AF9, but not including *Hoxa9*, *Mef2c*, or *Meis1*.

C/EBPα p42 Is a Myeloid Tumor Suppressor

The prevalence of *CEBPA* mutations leading to the specific loss of p42 in sporadic human AML (Leroy et al., 2005; Nerlov, 2004) and in the germline of familial AML pedigrees (Sellick et al., 2005; Smith et al., 2004) strongly indicated a role for such mutations in leukemogenesis. However, although complete inactivation of *Cebpa* in the hematopoietic system led to the accumulation of immature blasts in the bone marrow, no malignant disease resulted (Zhang et al., 2004). This is likely the result of a complete block in myeloid lineage formation, because GMPs fail to form in the absence of C/EBPα. Indeed, BCR-ABL, which normally induces transformation of the myeloid lineage, fails to induce AML in the absence of C/EBPα, but rather induces erythroleukemia (Wagner et al., 2006). p42-deficient myeloid cells are capable of myeloid lineage commitment, as evidenced by the formation of GMPs in L/L mice. Furthermore, BRM2 mice normally form GMPs and develop transformation of the myeloid lineage (Porse et al., 2005). Indeed, the phenotypic progression observed in L/L mice is similar to that seen in BRM2 mice, with initial neutropenia (L/L-1, BRM2-A phenotypes) succeeded by granulocyte hyperproliferation (L/L-2, BRM2-B phenotypes) and transformation (L/L-3, BRM2-C phenotypes), and we have shown that the BRM2-A and BRM2-B phenotypes progress to BRM2-C upon transplantation (Porse et al., 2005). Because p30 is deficient in E2F repression (Johansen et al., 2001), these observations are consistent with loss of C/EBPα-mediated E2F repression being an important component of the transformation process and being likely to drive the phenotypic progression, possibly by imposing selective pressure on the HSC compartment. Thus, selection for HSCs adapted to increased E2F activity by genetic or epigenetic means could allow the myeloblast that fail to survive in the LL-1 phenotype to differentiate, leading to the observed hyperproliferation of granulocytic cells. The high proliferative potential of myeloid progenitors in L/L mice is similar to that observed in BRM2 mice, indicating that the inability of p30 to repress E2F-dependent transcription also contributes directly to the increase in progenitor self-renewal capacity seen in the absence of p42. However, in the case of BRM2 mice, the transformed myeloid cells were not malignant. Overall, these results indicate that loss or retention of specific C/EBPα functions is required to induce malignant transformation of the myeloid lineage and, in particular, that the lineage instructive property of C/EBPα needs to be maintained for myeloid lineage transformation to occur and AML to develop. It is therefore of importance to develop genetically accurate models for *CEBPA* mutant AML to obtain clinically relevant mouse models.

The present data demonstrate that a knockin mutation that mimics the most prevalent *CEBPA* mutation observed in patients with AML causes myeloid leukemia with full penetrance in a mouse model. Our results provide direct genetic verification of the etiological relevance of these mutations and also demonstrate that the tumor suppressor activity of C/EBPα resides in the 42 kDa translational isoform. At the cellular level, our results show that efficient transformation of the granulocyte lineage observed in the absence of p42 is due to efficient p30-mediated bypass of the C/EBPα-dependent CMP-GMP transition, coupled with loss of proliferation control of the downstream myeloid progenitor population. In AML, specific loss of p42 may therefore be a means to circumnavigate the C/EBPα-controlled coupling of lineage commitment and proliferation control during myeloid differentiation, leading to the formation of progenitors with unchecked proliferative capacity and the ability to undergo transformation.

Table 1. Top 50 Coenriched Probe Sets in LL-LIC and L-GMP

Probe Set	Gene Symbol	Rank in Gene List	Rank Metric Score	Running ES	Self-Renewal Signature
1425180_at	SGIP1	6	8.092350006	0.02575028	
1418472_at	ASPA	8	7.616382122	0.0501929	
1425470_at	NA	10	7.364430904	0.07382548	yes
1425181_at	SGIP1	12	7.132127762	0.096711196	
1419609_at	CCR1	15	6.842639923	0.11862166	
1424186_at	CCDC80	19	6.723652363	0.14010505	
1450764_at	AOAH	30	5.84819603	0.15846215	
1452050_at	CAMK1D	35	5.585491657	0.17624177	yes
1419127_at	NPY	36	5.456165314	0.19378369	
1449924_at	PRG3	38	5.318623543	0.21083887	
1421681_at	NRG4	40	5.198602676	0.22750817	
1417614_at	CKM	45	5.031453133	0.24350652	
1425471_x_at	NA	49	4.875173092	0.25904694	yes
1451161_a_at	EMR1	50	4.84481287	0.2746233	
1449819_at	DMC1	52	4.79646492	0.28999972	
1418907_at	NA	59	4.535372734	0.3043141	
1420335_at	DMC1	65	4.377119541	0.3181642	
1416013_at	PLD3	79	4.21172142	0.33112636	yes
1437752_at	LIN28	94	3.97721839	0.34329006	
1426864_a_at	NCAM1	106	3.80211997	0.3550244	
1450109_s_at	ABCC2	118	3.669750929	0.36633313	
1426865_a_at	NCAM1	126	3.627708912	0.37768477	
1448162_at	VCAM1	128	3.613016605	0.38925633	
1425451_s_at	CHI3L3/CHI3L4	129	3.591151476	0.4008021	
1451972_at	GLCCI1	137	3.515051842	0.41179156	
1419610_at	CCR1	138	3.503375053	0.42305514	
1460719_a_at	P2RX1	139	3.501185894	0.43431166	yes
1448050_s_at	MAP4K4	140	3.469474077	0.44546625	yes
1454628_at	A930037G23RIK	141	3.46923852	0.45662007	
1460252_s_at	ZNF35	147	3.374240637	0.46724585	
1456195_x_at	ITGB5	150	3.332718134	0.4778717	yes
1417605_s_at	CAMK1	153	3.282420874	0.48833585	yes
1422760_at	PADI4	203	2.766919374	0.4950501	yes
1423702_at	H1F0	213	2.702160597	0.503337	
1425407_s_at	CLEC4A2/4B	225	2.626604557	0.511292	
1422013_at	CLEC4A2	237	2.562724113	0.51904154	
1419764_at	CHI3L3	261	2.355534792	0.5255908	
1418252_at	PADI2	268	2.326452494	0.5328033	
1427932_s_at	1200003I10RIK	295	2.189368725	0.5386847	
1419004_s_at	BCL2A1A/BCL2A1B	296	2.185925722	0.5457126	
1422818_at	NEDD9	298	2.175006866	0.5526608	
1425548_a_at	LST1	299	2.174248934	0.5596512	yes
1415866_at	UNC45A	316	2.122360468	0.56576234	
1424975_at	SIGLECF	320	2.106169701	0.5724003	
1425113_x_at	NA	326	2.077837706	0.578858	
1416759_at	MICAL1	330	2.064893246	0.5853632	
1454758_a_at	TSC22D1	346	1.989614367	0.59109217	
1422532_at	XPC	362	1.923462152	0.5966084	yes
1450522_a_at	H1F0	366	1.910332084	0.60261667	yes
1452657_at	AP1S2	371	1.906752586	0.6085689	

Loss of p42 Transforms Committed Myeloid Progenitors

The derivation of AML LICs from committed progenitors through transduction of AML-derived translocation products provided proof-of-principle that acquisition of leukemogenic potential may occur in a progenitor with limited proliferative potential. However, the use of viral transduction raises the issue of whether overexpression or ex vivo target cell selection influenced the results. By using a knockin approach, we have achieved the introduction of a common leukemogenic mutation in a manner that efficiently interrogates the entire hematopoietic hierarchy in its normal in vivo state, and where the oncogenic protein is expressed from its endogenous promoter. This led to the generation of LICs with a Mac1$^+$c-Kit$^+$ myeloid-committed immunophenotype that gave rise exclusively to myeloid cells in irradiated recipients, identifying them as transformed myeloid-restricted progenitor cells. These results indicate a propensity of *Cebpa* mutations to act on committed myeloid progenitors in vivo. As noted above, in studies of patients with AML patients who carried *CEBPA* mutations and who underwent complete remission and subsequent relapse, the initially observed *CEBPA* mutant alleles were almost uniformly present also in the relapse AML cells (Lin et al., 2005; Tiesmeier et al., 2003), indicating that *CEBPA* mutations are very early, possibly preleukemic, events in AML progression. Thus, although the nature of secondary genetic or epigenetic events contributing to cellular transformation in the L/L-3 mice remains to be determined, it is likely that our genetic model reflects the sequence of events normally occurring in human AML. By gene profiling of the LL-LIC population, we identified gene subsets that were consistently up- and downregulated in the transformed progenitors, and these genes were significantly enriched also in MLL-AF9-transformed L-GMPs. An important part of the transformation signature may therefore be determined by the target cell and the molecular properties of the differentiation program that has to be overridden by unlimited self-renewal. In contrast, overlap with the HSC-associated self-renewal signature was more limited; in particular, *Mef2c*, *Hoxa9*, and *Meis1* were all downregulated, suggesting that, although clearly important in the case of MLL-AF9-induced transformation, there is not a general requirement for their upregulation during progenitor transformation. This observation is consistent with upregulation of these genes in human AML being limited to those leukemias containing *MLL* translocations (Krivtsov et al., 2006). Conversely, we observed additional deregulation of the C/EBP complex (i.e., upregulation of *Ddit3*/*Cebpz* and downregulation of *Cebpb*), which is a trait not shared with the MLL-AF9-transformed progenitors. Thus, common and initiator mutation-specific traits may coexist in leukemic progenitor populations, and both may be required for transformed to occur. It is interesting that the LIC activity was detected in the Mac-1$^+$c-Kit$^+$ fraction C, but not in the Mac-1$^{-/lo}$c-Kit$^+$ fraction B. This could be due to either lower frequency of LICs in the latter population or a role for Mac-1 or other adhesion molecules differentially expressed on these populations in homing of LICs to an appropriate location. This is currently being investigated.

How do we reconcile the data obtained in murine genetic and viral transduction experiments defining LICs as bipotent or committed myeloid progenitors with those obtained by NOD/SCID transplantation of human AML cells, where LICs were cells with a CD34$^+$CD38$^-$ phenotype, similar to that of normal SCID-repopulating HSCs (Bonnet and Dick, 1997; Lapidot et al., 1994)? First, it should be noted that the murine model system is able to model AML based in the LSK compartment, as exemplified by the disease observed in mice carrying knockdown mutations in the *Sfpi1* gene, which encodes the PU.1 transcription factor (Steidl et al., 2006). Second, 30%–50% of human AML cases do not engraft in NOD/SCID mice, and the capacity to engraft has been found to correlate with adverse prognosis (Monaco et al., 2004; Pearce et al., 2006). This would be consistent with a distinct type of LICs, which are more responsive to current treatment protocols but are not able to engraft in the current NOD/SCID model, being present in patients with good prognosis. A self-renewing and proliferative myeloid progenitor would be a candidate for such an LIC. This is a possibility that is currently being tested and that could have a significant impact on AML treatment should it become feasible to prospectively identify distinct types of patient LICs.

EXPERIMENTAL PROCEDURES

Generation and Maintenance of *Cebpa* p42 Knockout Mice

p42 knockout mice were generated by standard techniques. Details are provided in the Supplemental Experimental Procedures. Mice were maintained on standard chow under specific pathogen free conditions on a 75% C57BL/6, 25% 129/Ola background for all experiments, and littermates were used as controls. Mice were monitored by peripheral blood analysis and were considered moribund when they were severely anemic; this in all cases correlated with the presence of disseminated disease. Animal experiments were approved by the EMBL Monterotondo Ethical Committee and were performed according to EMBL institutional and Italian national guidelines.

Blood and Hematopoietic Tissue Analysis

Mice were tail bled, and peripheral blood counts were performed using a Hemavet 950 (Drew Scientific) calibrated for mouse blood. Flow cytometry was performed as described elsewhere (Kirstetter et al., 2006; Porse et al., 2005). For cell cycle analysis, BrdU incorporation was detected by flow cytometry using the BrdU Flow Kit (PharMingen), according to the manufacturer's instructions. BrdU labeling was for 2 hr before death. Differential counts were performed as described elsewhere (Porse et al., 2005).

Histology

Sections of liver or adipose tissue were prepared as described elsewhere (Porse et al., 2001) and were stained with hematoxylin-eosin or were used for immunohistochemistry using rabbit anti-MPO (A0398; DAKO) or rabbit anti-NGAL (Kjeldsen et al., 1996) as primary antibody. Binding of primary antibodies was detected using an Envision+ HRP (DAB) detection kit (DAKO),

The table shows the top 50 probe sets providing the core enrichment of LL-LIC upregulated genes in L-GMPs (six samples), compared with normal GMP (four samples) (Krivtsov et al., 2006). All MOE430A probe sets (22691) were ranked according to their expression in L-GMP versus normal progenitors using the GSEA algorithm. The probe sets shown are the 50 highest contributors to the positive enrichment score (leading edge). The rank of the probe sets (in L-GMP/GMP comparison), the running enrichment score (ES), and the probe sets present in the MLL-AF9 and HSC-derived self-renewal signature (Krivtsov et al., 2006) are indicated. NA, not annotated.

according to the manufacturer's recommendations. After that, the sections were counterstained with hematoxylin.

Tissue Culture and Colony Assays

Colony assays were performed as described elsewhere (Porse et al., 2005). Immortalized L/L cells were grown in DMEM plus 10% FCS (Invitrogen) supplemented with 50 ng/ml SCF, 10 ng/ml IL-6, and 10 ng/ml IL-3 (Sigma). For analysis of factor dependence, 5×10^3 cells were washed and plated in the same medium, omitting the indicated factor, and live cells were counted after 3 and 6 days.

Western Blotting

Nuclear lysate was prepared from approximately 200 mg of liver by homogenization in 15 ml of hypotonic buffer (10 mM HEPES [pH 7.9], 1.5 mM $MgCl_2$, 10 mM KCl, and 0.5 mM DTT) using a Dounce homogenizer (B-type pestle, 10 strokes); liver was left on ice for 10 min to allow any clumps to settle. Nuclei were collected by centrifugation (20 min, 450 g), were resuspended in 300 μl of PBS, and were lysed by addition of 300 μl of SDS loading buffer (250 mM Tris-Cl [pH 6.8], 40% sucrose, 12% SDS, and 6% β-mercaptoethanol) and boiling. Western blotting was performed as described elsewhere (Porse et al., 2001) using 14AA rabbit anti-C/EBPα antibody (sc-61; Santa Cruz Biotechnology), mouse antitubulin (T9026; Sigma), and mouse anti-β-actin (A4700; Sigma).

FACS Analysis, Cell Separation, and Cell Sorting

Antibodies were obtained from PharMingen or eBioscience. Flow cytometric analysis was performed as described elsewhere (Kirstetter et al., 2006; Porse et al., 2005). Magnetic-activated cell separation (MACS; Miltenyi Biotech) was performed by labeling with biotinylated anti-Mac-1 (CD11b; clone M1/70) and streptavidin coupling to paramagnetic beads (Miltenyi Biotec), as recommended by the manufacturer. For cell sorting, BM cells were subjected to immunomagnetic-based pre-enrichment using a biotinylated-conjugated lineage cocktail containing CD4 (RM4-5), CD8 (53-6), B220 (RA3-6B2), CD5 (53-7.3), and Ter119 (Ly-76). Lin^{*-} cells were incubated with Sav-PE-Cy5, Sca-1-PE-Cy7, c-Kit-APC, and Mac-1-FITC. A FACSAria cell sorter (Becton Dickinson) was used for sorting fractions A, B, C, and D from L/+ and L/L-3 mice. LSK, GMP, and MEP staining was performed as described elsewhere (Kirstetter et al., 2006). Sorting was performed using a FACSAria cell sorter.

SKY

For SKY, primary tumor cells were cultured in M3434 medium and were processed as described elsewhere (Schrock et al., 1996).

Bone Marrow Transplantation

Recipient mice were exposed to 5.5 Gy total-body X-irradiation 6 hr before BM transplantation. For transplantation of magnetically enriched cells, CD45.1/2 recipients received 4×10^5 C57BL/6-CD45.1 competitor total BM cells and 1×10^5 CD45.2 cells from L/+ or L/L mice. For transplantation of sorted cells, CD45.1 recipients received 2.5×10^5 CD45.1/2 competitor total BM cells with 2×10^3 CD45.2 cells from fraction A, B, C, or D from L/+ or L/L-3 mice. Determination of donor/competitor contribution and lineage contribution was determined as described elsewhere (Kirstetter et al., 2006).

Microarray Analysis and Statistical Analysis

For details of microarray data analysis, see the Supplemental Experimental Procedures.

GSEA was performed as described elsewhere (Subramanian et al., 2005), using the GSEA 2.0 algorithm (http://www.broad.mit.edu/gsea). Ranked expression lists of up- or downregulated genes derived from the analysis of LL-LIC and control arrays were used as gene sets, and their enrichment was tested in a data set consisting of arrays from L-GMP and GMP samples (Krivtsov et al., 2006), where genes were ranked on the basis of Student's t test. Statistical significance was determined using Student's t test, except for significance of differences in survival, where the log-rank test was used.

ACCESSION NUMBERS

The microarray data generated in this study are deposited in the European Bioinformatics Institute ArrayExpress database (http://www.ebi.ac.uk/arrayexpress) with the accession number E-MEXP-1444.

SUPPLEMENTAL DATA

The Supplemental Data include Supplemental Experimental Procedures, eight supplemental figures, and two supplemental tables and can be found with this article online at http://www.cancercell.org/cgi/content/full/13/4/299/DC1/.

ACKNOWLEDGMENTS

The authors thank L. Friis-Hansen and B. Lindberg for histology, N. Borregaard for anti-Ngal antibody, and A. Frensel and P. Freitag for expert molecular cytogenetic assistance. This work was supported by the European Commission (EuroCSC STREP), the Association for International Cancer Research, the Associazione Italiana per la Ricerca sul Cancro, the Danish Cancer Society, the Danish Medical Research Council, the Danish Research Agency, the Novo-Nordisk Foundation, and the HematoLinne strategic grant from the Swedish Research Council.

Received: June 26, 2007
Revised: December 19, 2007
Accepted: February 12, 2008
Published: April 7, 2008

REFERENCES

Ayton, P.M., and Cleary, M.L. (2003). Transformation of myeloid progenitors by MLL oncoproteins is dependent on Hoxa7 and Hoxa9. Genes Dev. *17*, 2298–2307.

Bonnet, D., and Dick, J.E. (1997). Human acute myeloid leukemia is organized as a hierarchy that originates from a primitive hematopoietic cell. Nat. Med. *3*, 730–737.

Cozzio, A., Passegue, E., Ayton, P.M., Karsunky, H., Cleary, M.L., and Weissman, I.L. (2003). Similar MLL-associated leukemias arising from self-renewing stem cells and short-lived myeloid progenitors. Genes Dev. *17*, 3029–3035.

Frohling, S., Schlenk, R.F., Stolze, I., Bihlmayr, J., Benner, A., Kreitmeier, S., Tobis, K., Dohner, H., and Dohner, K. (2004). CEBPA mutations in younger adults with acute myeloid leukemia and normal cytogenetics: prognostic relevance and analysis of cooperating mutations. J. Clin. Oncol. *22*, 624–633.

Heath, V., Suh, H.C., Holman, M., Renn, K., Gooya, J.M., Parkin, S., Klarmann, K.D., Ortiz, M., Johnson, P., and Keller, J. (2004). C/EBPα deficiency results in hyperproliferation of hematopoietic progenitor cells and disrupts macrophage development in vitro and in vivo. Blood *104*, 1639–1647.

Huntly, B.J., Shigematsu, H., Deguchi, K., Lee, B.H., Mizuno, S., Duclos, N., Rowan, R., Amaral, S., Curley, D., Williams, I.R., et al. (2004). MOZ-TIF2, but not BCR-ABL, confers properties of leukemic stem cells to committed murine hematopoietic progenitors. Cancer Cell *6*, 587–596.

Johansen, L.M., Iwama, A., Lodie, T.A., Sasaki, K., Felsher, D.W., Golub, T.R., and Tenen, D.G. (2001). c-Myc is a critical target for C/EBPα in granulopoiesis. Mol. Cell. Biol. *21*, 3789–3806.

Kirstetter, P., Anderson, K., Porse, B.T., Jacobsen, S.E., and Nerlov, C. (2006). Activation of the canonical Wnt pathway leads to loss of hematopoietic stem cell repopulation and multilineage differentiation block. Nat. Immunol. *7*, 1048–1056.

Kjeldsen, L., Koch, C., Arnljots, K., and Borregaard, N. (1996). Characterization of two ELISAs for NGAL, a newly described lipocalin in human neutrophils. J. Immunol. Methods *198*, 155–164.

Kottaridis, P.D., Gale, R.E., Langabeer, S.E., Frew, M.E., Bowen, D.T., and Linch, D.C. (2002). Studies of FLT3 mutations in paired presentation and relapse samples from patients with acute myeloid leukemia: implications for the role of FLT3 mutations in leukemogenesis, minimal residual disease detection, and possible therapy with FLT3 inhibitors. Blood *100*, 2393–2398.

Krivtsov, A.V., Twomey, D., Feng, Z., Stubbs, M.C., Wang, Y., Faber, J., Levine, J.E., Wang, J., Hahn, W.C., Gilliland, D.G., et al. (2006). Transformation from committed progenitor to leukaemia stem cell initiated by MLL-AF9. Nature *442*, 818–822.

Lapidot, T., Sirard, C., Vormoor, J., Murdoch, B., Hoang, T., Caceres-Cortes, J., Minden, M., Paterson, B., Caligiuri, M.A., and Dick, J.E. (1994). A cell initiating human acute myeloid leukaemia after transplantation into SCID mice. Nature *367*, 645–648.

Leroy, H., Roumier, C., Huyghe, P., Biggio, V., Fenaux, P., and Preudhomme, C. (2005). CEBPA point mutations in hematological malignancies. Leukemia *19*, 329–334.

Lin, F.T., MacDougald, O.A., Diehl, A.M., and Lane, M.D. (1993). A 30-kDa alternative translation product of the CCAAT/enhancer binding protein α message: transcriptional activator lacking antimitotic activity. Proc. Natl. Acad. Sci. USA *90*, 9606–9610.

Lin, L.I., Chen, C.Y., Lin, D.T., Tsay, W., Tang, J.L., Yeh, Y.C., Shen, H.L., Su, F.H., Yao, M., Huang, S.Y., et al. (2005). Characterization of CEBPA mutations in acute myeloid leukemia: most patients with CEBPA mutations have biallelic mutations and show a distinct immunophenotype of the leukemic cells. Clin. Cancer Res. *11*, 1372–1379.

Monaco, G., Konopleva, M., Munsell, M., Leysath, C., Wang, R.Y., Jackson, C.E., Korbling, M., Estey, E., Belmont, J., and Andreeff, M. (2004). Engraftment of acute myeloid leukemia in NOD/SCID mice is independent of CXCR4 and predicts poor patient survival. Stem Cells *22*, 188–201.

Nerlov, C. (2004). C/EBPα mutations in acute myeloid leukaemias. Nat. Rev. Cancer *4*, 394–400.

Pabst, T., Mueller, B.U., Zhang, P., Radomska, H.S., Narravula, S., Schnittger, S., Behre, G., Hiddemann, W., and Tenen, D.G. (2001). Dominant-negative mutations of CEBPA, encoding CCAAT/enhancer binding protein-α (C/EBPα), in acute myeloid leukemia. Nat. Genet. *27*, 263–270.

Pearce, D.J., Taussig, D., Zibara, K., Smith, L.L., Ridler, C.M., Preudhomme, C., Young, B.D., Rohatiner, A.Z., Lister, T.A., and Bonnet, D. (2006). AML engraftment in the NOD/SCID assay reflects the outcome of AML: implications for our understanding of the heterogeneity of AML. Blood *107*, 1166–1173.

Porse, B.T., Pedersen, T.A., Xu, X., Lindberg, B., Wewer, U.M., Friis-Hansen, L., and Nerlov, C. (2001). E2F repression by C/EBPα is required for adipogenesis and granulopoiesis in vivo. Cell *107*, 247–258.

Porse, B.T., Bryder, D., Theilgaard-Monch, K., Hasemann, M.S., Anderson, K., Damgaard, I., Jacobsen, S.E., and Nerlov, C. (2005). Loss of C/EBPα cell cycle control increases myeloid progenitor proliferation and transforms the neutrophil granulocyte lineage. J. Exp. Med. *202*, 85–96.

Schrock, E., du Manoir, S., Veldman, T., Schoell, B., Wienberg, J., Ferguson-Smith, M.A., Ning, Y., Ledbetter, D.H., Bar-Am, I., Soenksen, D., Garini, Y., et al. (1996). Multicolor spectral karyotyping of human chromosomes. Science *273*, 494–497.

Sellick, G.S., Spendlove, H.E., Catovsky, D., Pritchard-Jones, K., and Houlston, R.S. (2005). Further evidence that germline CEBPA mutations cause dominant inheritance of acute myeloid leukaemia. Leukemia *19*, 1276–1278.

Shih, L.Y., Huang, C.F., Wu, J.H., Lin, T.L., Dunn, P., Wang, P.N., Kuo, M.C., Lai, C.L., and Hsu, H.C. (2002). Internal tandem duplication of FLT3 in relapsed acute myeloid leukemia: a comparative analysis of bone marrow samples from 108 adult patients at diagnosis and relapse. Blood *100*, 2387–2392.

Shih, L.Y., Liang, D.C., Huang, C.F., Wu, J.H., Lin, T.L., Wang, P.N., Dunn, P., Kuo, M.C., and Tang, T.C. (2006). AML patients with CEBPα mutations mostly retain identical mutant patterns but frequently change in allelic distribution at relapse: a comparative analysis on paired diagnosis and relapse samples. Leukemia *20*, 604–609.

Smith, M.L., Cavenagh, J.D., Lister, T.A., and Fitzgibbon, J. (2004). Mutation of CEBPA in familial acute myeloid leukemia. N. Engl. J. Med. *351*, 2403–2407.

Somervaille, T.C., and Cleary, M.L. (2006). Identification and characterization of leukemia stem cells in murine MLL-AF9 acute myeloid leukemia. Cancer Cell *10*, 257–268.

Steidl, U., Rosenbauer, F., Verhaak, R.G., Gu, X., Ebralidze, A., Otu, H.H., Klippel, S., Steidl, C., Bruns, I., Costa, D.B., et al. (2006). Essential role of Jun family transcription factors in PU.1 knockdown-induced leukemic stem cells. Nat. Genet. *38*, 1269–1277.

Subramanian, A., Tamayo, P., Mootha, V.K., Mukherjee, S., Ebert, B.L., Gillette, M.A., Paulovich, A., Pomeroy, S.L., Golub, T.R., Lander, E.S., et al. (2005). Gene set enrichment analysis: a knowledge-based approach for interpreting genome-wide expression profiles. Proc. Natl. Acad. Sci. USA *102*, 15545–15550.

Tiesmeier, J., Czwalinna, A., Muller-Tidow, C., Krauter, J., Serve, H., Heil, G., Ganser, A., and Verbeek, W. (2003). Evidence for allelic evolution of C/EBPα mutations in acute myeloid leukaemia. Br. J. Haematol. *123*, 413–419.

Wagner, K., Zhang, P., Rosenbauer, F., Drescher, B., Kobayashi, S., Radomska, H.S., Kutok, J.L., Gilliland, D.G., Krauter, J., and Tenen, D.G. (2006). Absence of the transcription factor CCAAT enhancer binding protein α results in loss of myeloid identity in bcr/abl-induced malignancy. Proc. Natl. Acad. Sci. USA *103*, 6338–6343.

Wang, N.D., Finegold, M.J., Bradley, A., Ou, C.N., Abdelsayed, S.V., Wilde, M.D., Taylor, L.R., Wilson, D.R., and Darlington, G.J. (1995). Impaired energy homeostasis in C/EBPα knockout mice. Science *269*, 1108–1112.

Wiktor, A., Rybicki, B.A., Piao, Z.S., Shurafa, M., Barthel, B., Maeda, K., and Van Dyke, D.L. (2000). Clinical significance of Y chromosome loss in hematologic disease. Genes Chromosomes Cancer *27*, 11–16.

Wong, P., Iwasaki, M., Somervaille, T.C., So, C.W., and Cleary, M.L. (2007). Meis1 is an essential and rate-limiting regulator of MLL leukemia stem cell potential. Genes Dev. *21*, 2762–2774.

Zhang, D.E., Zhang, P., Wang, N.D., Hetherington, C.J., Darlington, G.J., and Tenen, D.G. (1997). Absence of granulocyte colony-stimulating factor signaling and neutrophil development in CCAAT enhancer binding protein α-deficient mice. Proc. Natl. Acad. Sci. USA *94*, 569–574.

Zhang, P., Iwasaki-Arai, J., Iwasaki, H., Fenyus, M.L., Dayaram, T., Owens, B.M., Shigematsu, H., Levantini, E., Huettner, C.S., Lekstrom-Himes, J.A., et al. (2004). Enhancement of hematopoietic stem cell repopulating capacity and self-renewal in the absence of the transcription factor C/EBPα. Immunity *21*, 853–863.